

# Anomalies in multiline-TRL-corrected measurements of short CPW lines

Gia Ngoc Phung and Uwe Arz

Physikalisch-Technische Bundesanstalt, PTB - Bundesallee 100, 38116 Braunschweig, Germany

**Abstract**—Microwave probes in on-wafer measurements contribute to a number of parasitic effects deteriorating the accuracy of multiline Thru Reflect Line (mTRL) calibrations. The accuracy of mTRL calibration is especially sensitive in Devices under Test (DUTs) of shorter line length. It has been demonstrated in previous experimental studies that the calibrated results are often only reliable as long as the length of the line is at least 2 mm. However, the reasons behind this phenomenon have not yet been clarified. Therefore, this paper reports on a systematic analysis of the dependency of the mTRL calibration accuracy on probe effects with a focus on coplanar waveguides (CPW) of shorter line length. For the first time, investigations with regard to the probe effects in shorter CPWs are presented.

**Index Terms**—calibration, coplanar waveguides, on-wafer, probes.

## I. INTRODUCTION

On-wafer measurements are essential for the characterization of active and passive components in many applications ranging from wireless communications, automotive radar and medical sensing. They have been known as ambitious and challenging containing a lot of parasitic effects degrading the accuracy of calibrated results. It has been found that the influence of probe geometries has a significant impact on the accuracy of the multiline Thru Reflect Line (mTRL)-calibrated on-wafer measurements. In [1] investigations concerning the influence of microwave probes on calibrated on-wafer measurements are presented for coplanar waveguides (CPW) and thin-film microstrip lines (TFMSL) up to W-Band. Similar investigations have been demonstrated in [2] and [3] for the extended frequency range up to 500 GHz. In [4] experimental studies have demonstrated that the calibrated results are only reliable for line lengths of at least 2 mm. The accuracy of mTRL calibration is severely impaired for Devices under Test (DUTs) of shorter line length. However the reason for this has not yet been clarified. With this motivation, this paper demonstrates the dependency of the mTRL calibration accuracy on probe effects with a focus on CPWs of shorter line length. The goal of this paper to close this gap and to clarify the underlying phenomena of the probe influences for CPWs of shorter line length. Starting from a measurement example, this paper presents a systematic study of how the mTRL-calibrated S-parameters of the CPW change with the line length.

All results presented here, both simulated and measured ones, have been processed with a mTRL calibration according to [5]. The calibration set consists of a short as reflect, a 400  $\mu\text{m}$  long CPW line as thru and a selection of seven additional lines with lengths of 500, 700, 900, 2400, 5400, 7400 and 11400  $\mu\text{m}$ . The parameters of the CPW cross section are the signal width  $w = 62 \mu\text{m}$ , the gap width  $s = 6 \mu\text{m}$ , the

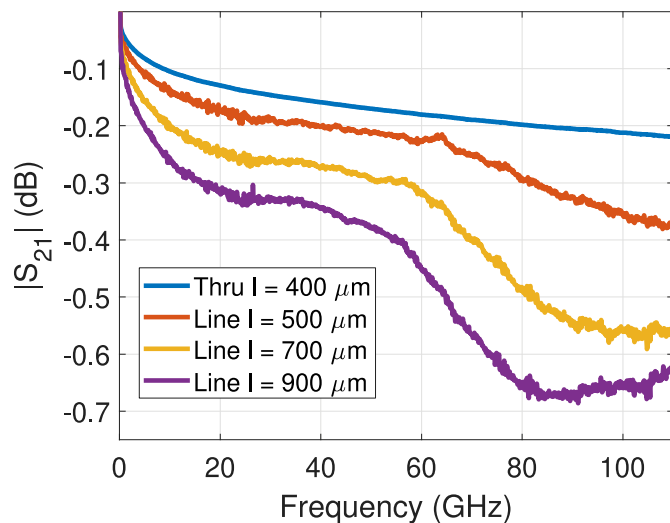


Fig. 1. Magnitude of measured mTRL-calibrated transmission coefficient  $S_{21}$  for CPWs of different lengths  $l$ .

metal ground width  $w_g = 250 \mu\text{m}$  and the metal thickness  $t = 0.534 \mu\text{m}$  on fused silica substrate ( $\epsilon_r = 3.78$ ), which has been used in [6]. The layout of the wafer has been investigated, designed and manufactured with large spacing between the elements to mitigate the impact of probe coupling due to neighboring effects [7]. All the measurements were performed with GGB probes with a 100  $\mu\text{m}$  pitch. To avoid multimode propagation the measurements were performed on a ceramic chuck (with a permittivity  $\epsilon_{r, \text{chuck}} = 6.5$  larger than that of the wafer  $\epsilon_r = 3.78$ , see [6] and [7]). For the electromagnetic simulations, CST Studio Suite from Dassault Systemes was applied [8]. To enable comparisons of simulations against measurements, the reference plane of the calibration was shifted to the probe tips.

## II. INFLUENCE OF PROBE PROPERTIES ON SHORT CPW STRUCTURES

### A. Measurement results

Fig. 1 shows the mTRL-calibrated measurements of the transmission coefficient magnitude of CPW lines of different lengths  $l$  ranging from 400 to 900  $\mu\text{m}$ . The line lengths from 500 to 900  $\mu\text{m}$  shown in Fig. 1 were treated as DUTs, therefore they were not part of the mTRL calibration set. Obviously, all the measurements except the Thru standard reveal distinct peculiarities. Up to 30 GHz a smooth curve behavior can be detected. Beyond 30 GHz all the measurements except the Thru standard show a wavy curve behavior which then turns into a local minimum or dip behavior.

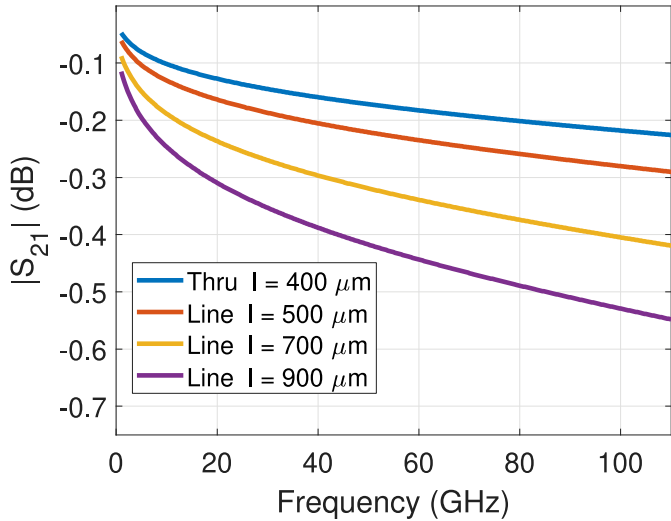


Fig. 2. mTRL-calibrated transmission coefficient  $S_{21}$  for CPWs of different lengths  $l$  using data calculated by the CPW model of [9].

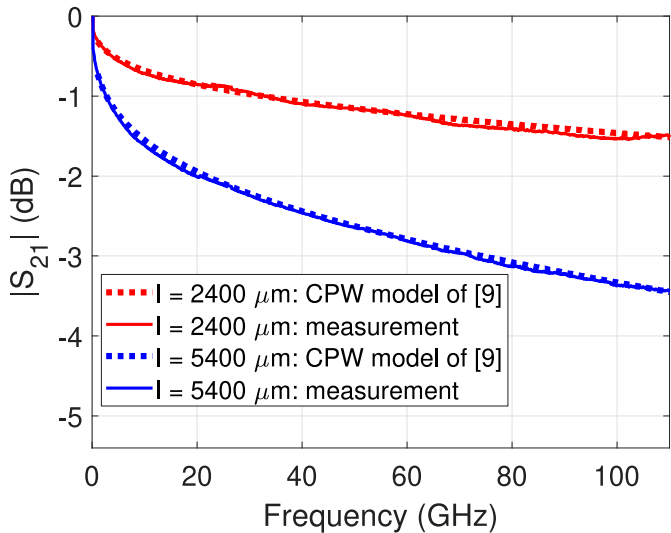


Fig. 3. Comparison between CPW model of [9] and measurements for the CPW with  $l = 2400 \mu\text{m}$  and  $l = 5400 \mu\text{m}$ .

The first question to clarify is whether this behavior is an artifact stemming from numerical inaccuracies of the mTRL calibration or a physical effect caused by parasitics. Thus, to clarify this behavior, the transmission coefficient  $S_{21}$  of the CPWs is calculated by the analytical model of [9]. The CPW model of [9] represents an ideal case without any disturbances due to probe effects. To ensure consistency, the calculated data from the CPW model of [9] is also processed with the mTRL calibration. The calibrated results are plotted in Fig. 2. As expected, all the calibrated data do not reveal any peculiarities and show a smooth ideal curve behavior over the whole frequency range.

When comparing the measured transmission coefficient  $S_{21}$  of longer CPWs against the CPW model results (Fig. 3),

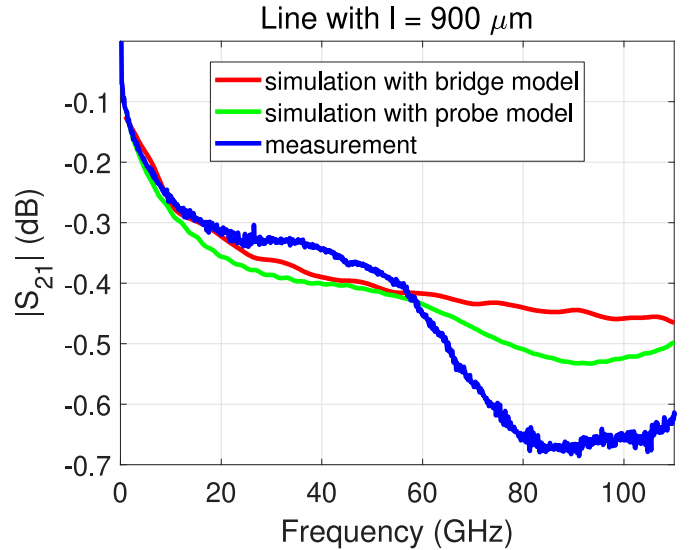


Fig. 4. Calibrated results of the transmission coefficient  $S_{21}$  for the CPW of  $l = 900 \mu\text{m}$ .

interestingly the dip behavior observed in Fig. 1 fades away when the CPW length is increased. In both cases, the transmission coefficients are approaching that of the CPW model of [9]. Overall, there is only a small discrepancy between the measurements and the CPW model of [9]. This proves that the dip behavior observed in the short CPWs is not an artifact stemming from numerical inaccuracies of the mTRL calibration since the calibrated data of the CPW model of [9] does not reveal any peculiarities and shows the ideal behavior (true performance) of the CPW.

#### B. Comparison with simulation results from different excitations

Due to the layout of the wafer which has been designed to avoid neighboring effects and to ensure single-mode CPW propagation (following the guidelines of [7]), the underlying phenomena could only be attributed to the non-idealities of the probe influence. To clarify this behavior electromagnetic simulations using two different excitations, the probe model (used in [10] and [1]) and the bridge model (implemented in [11]) are added. The probe model describes a sophisticated model emulating the real measurement probe properties whereas the bridge model represents an almost ideal excitation with the least possible parasitic effects. In order to reproduce the measurement results, the entire wafer was modelled in CST and the simulations of the complete calibration set were performed with the two different excitations.

The results shown in Figs. 4, 5 and 6 clearly demonstrate that the bridge excitation reveals a smooth curve behavior for all the line lengths and is comparable to the CPW model of [9]. The probe model on the other hand exhibits divergent behavior. For the CPW length of  $l = 900 \mu\text{m}$  the probe model shows the expected dip behavior similar to the measurement (Fig. 4). With longer CPW lengths the dip behavior disappears

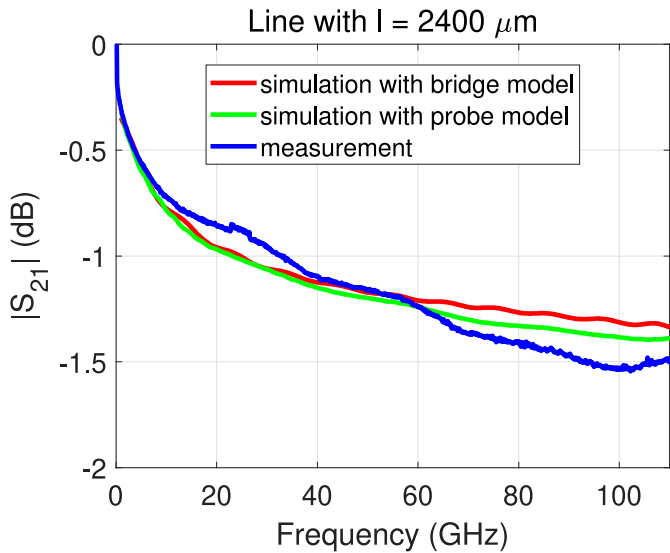


Fig. 5. Calibrated results of the transmission coefficient  $S_{21}$  for the CPW of  $l = 2400 \mu\text{m}$ .

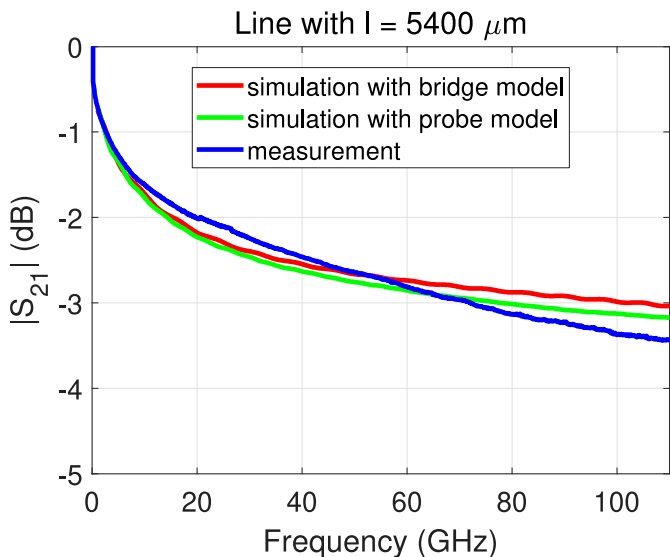


Fig. 6. Calibrated results of the transmission coefficient  $S_{21}$  for the CPW of  $l = 5400 \mu\text{m}$ .

in the simulation results as well as in the measurement results. Whereas the CPW with  $l = 2400 \mu\text{m}$  still shows a slightly wavy curve behavior, the waviness has disappeared in the transmission coefficient  $S_{21}$  of the CPW with  $l = 5400 \mu\text{m}$ . Within this frequency range and for the investigated CPW dimensions, the transversal dimensions are still small compared to the wavelength and thus radiation effects are not dominating. Therefore, the results of the CPW lines would only follow a smooth square root function of the frequency, comparable to the results calculated by the CPW model of [9]. However, the results demonstrate that this statement is only valid for longer CPWs. As long as the line length is below 2 mm, the curve behavior does not follow the expected smooth

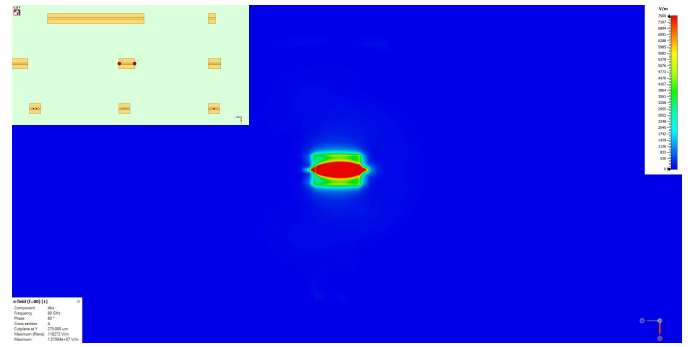


Fig. 7. Top view: Simulated electric fields of the complete wafer with bridge model for the CPW with length of  $l = 900 \mu\text{m}$  at  $f = 80 \text{ GHz}$ .

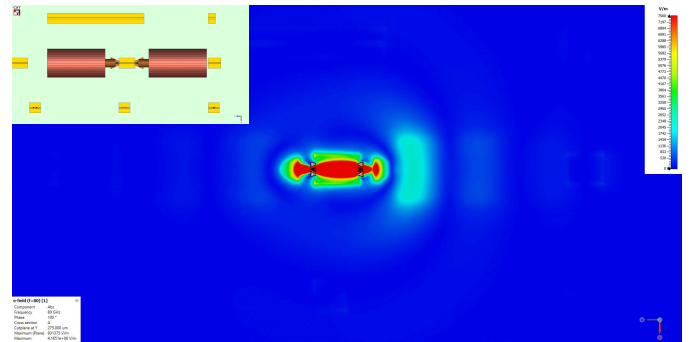


Fig. 8. Top view: Simulated electric fields of the complete wafer with probe model for the CPW with length of  $l = 900 \mu\text{m}$  at  $f = 80 \text{ GHz}$ .

function any more. This indicates that even for a wafer layout designed with minimal parasitics the mTRL calibration cannot completely compensate for the probe influence in short CPW lengths.

### C. Field plots

The field plots in Fig. 7 and Fig. 8 confirm the above statement. For both excitations, neither the crosstalk behavior between adjacent structures nor probe coupling with neighboring structures are responsible for the peculiarities detected in the measurement result of CPWs in Fig. 1.

Obviously, the neighboring structures surrounding the DUT are less coupled due to the large distances between each element. There is also no clear indication of interference with multimode or substrate modes propagation. What is more important to note is that the fields at the probe contact (Fig. 8) differ from that of the bridge model (Fig. 7). One can observe stray fields at the edge of the CPW and around the regions below the probe needles in Fig. 8. The transition from the probe needles to the coplanar pads causes field discontinuities. Thus, coupling between the probes is also increased (Fig. 9). Fig. 9 shows the cross-sectional view of the simulated electric fields for the CPW lengths of  $l = 500, 900$  and  $2400 \mu\text{m}$  to illustrate this behavior. Due to the shorter CPW length the energy is not only transmitted through the CPW path but also over the air through the probe needles, see e.g. Fig. 9,  $l = 900 \mu\text{m}$ . Depending on the CPW line length the

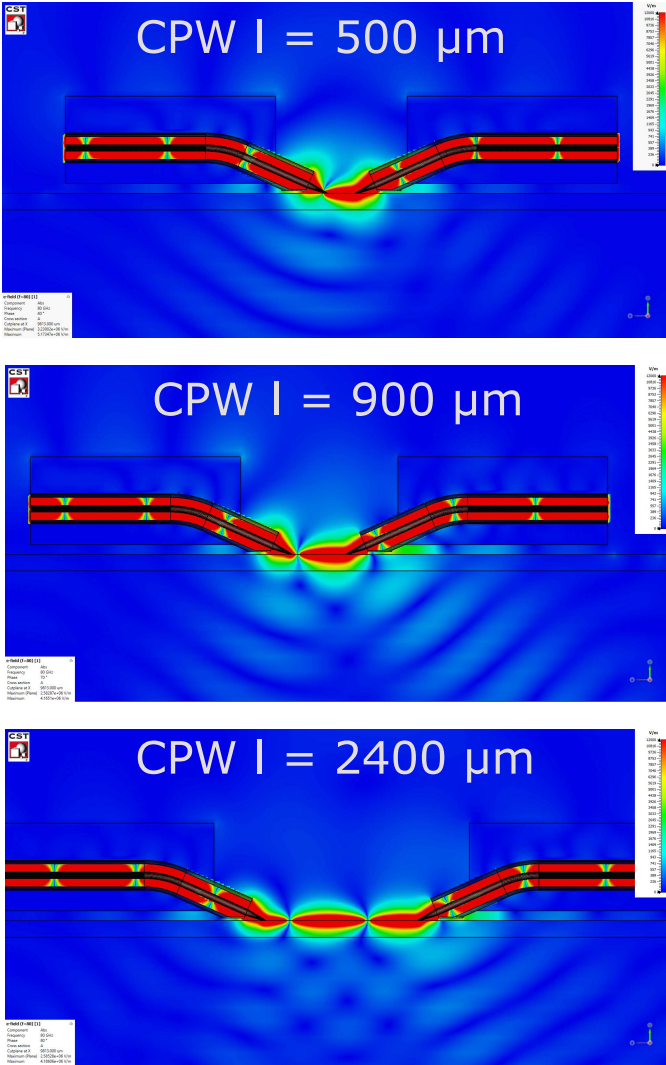


Fig. 9. Cross-sectional view: Simulated electric fields of the complete wafer with probe model for the CPW with length of  $l = 500, 900$  and  $2400 \mu\text{m}$  at  $f = 80 \text{ GHz}$ .

probe coupling between the needles differs and thus the field distribution in the air around the probe needles also changes. This divergent field distribution which varies with CPW line length cannot be fully compensated by the mTRL calibration. Thus, this results in distinct peculiarities observed in the transmission coefficient  $S_{21}$  of the short CPW structures. For the investigated probe type this effect documents itself in a dip behavior detected in the measurements (Fig. 1). So therefore one can state that this effect is a mTRL-calibration artifact in combination with the probe effects. Further investigations revealed that for other probe types this effect also occurs, however with a different dip behavior.

### III. CONCLUSION

Summarizing the above results, one can state that the mTRL calibration cannot fully compensate for the coupling between the probe needles in CPWs of shorter line length. This effect

leads to distinct peculiarities which document themselves in a dip behavior detected in the mTRL-calibrated measurements. As long as the CPW line length exceeds 2 mm, the effect becomes negligible.

### ACKNOWLEDGMENT

The authors acknowledge support by the European Metrology Programme for Innovation and Research (EMPIR) Project 14IND02 “Microwave measurements for planar circuits and components”. Furthermore, this work was supported in part by 18SIB09 “Traceability for electrical measurements at millimetre-wave and terahertz frequencies for communications and electronics technologies”.

Both projects (14IND02 and 18SIB09) have received funding from the EMPIR programme co-financed by the Participating States and from the European Union’s Horizon 2020 research and innovation programme.

The authors are also grateful to Rohde & Schwarz for manufacturing the calibration substrate.

### REFERENCES

- [1] G. N. Phung, F. J. Schmückle, R. Doerner, B. Kähne, T. Fritzsche, U. Arz, and W. Heinrich, “Influence of Microwave Probes on Calibrated On-Wafer Measurements,” *IEEE Transactions on Microwave Theory and Techniques*, vol. 67, no. 5, pp. 1892–1900, 2019.
- [2] S. Fregonese, M. De matos, M. Deng, M. Potereau, C. Ayela, K. Aufinger, and T. Zimmer, “On-Wafer Characterization of Silicon Transistors Up To 500 GHz and Analysis of Measurement Discontinuities Between the Frequency Bands,” *IEEE Transactions on Microwave Theory and Techniques*, vol. 66, no. 7, pp. 3332–3341, 2018.
- [3] C. Yadav, M. Deng, S. Fregonese, M. Cabbia, M. De Matos, B. Plano, and T. Zimmer, “Importance and Requirement of Frequency Band Specific RF Probes EM Models in Sub-THz and THz Measurements up to 500 GHz,” *IEEE Transactions on Terahertz Science and Technology*, vol. 10, no. 5, pp. 558–563, 2020.
- [4] S. Amakawa, A. Orii, K. Katayama, K. Takano, M. Motoyoshi, T. Yoshida, and M. Fujishima, “Design of Well-behaved Low-loss Millimetre-wave CMOS Transmission Lines,” in *2014 IEEE 18th Workshop on Signal and Power Integrity (SPI)*, 2014, pp. 1–4.
- [5] R. B. Marks, “A Multiline Method of Network Analyzer Calibration,” *IEEE Trans. on Microwave Theory and Techniques*, vol. 39, no. 7, pp. 1205–1215, 1991.
- [6] U. Arz, K. Kuhlmann, T. Dziomba, G. Hechtfisher, G. N. Phung, F. J. Schmückle, and W. Heinrich, “Traceable Coplanar Waveguide Calibrations on Fused Silica Substrates up to 110 GHz,” *IEEE Transactions on Microwave Theory and Techniques*, vol. 67, no. 6, pp. 2423–2432, 2019.
- [7] M. Spirito, U. Arz, G. N. Phung, F. J. Schmückle, W. Heinrich, and R. Lozar, “Guidelines for the Design of Calibration Substrates, including the Suppression of Parasitic Modes for Frequencies up to and including 325 GHz,” *EMPIR 14IND02 – PlanarCal, 2018, Physikalisch-Technische Bundesanstalt (PTB)*, 2018.
- [8] “CST Studio Suite,” 2020. [Online]. Available: <https://www.3ds.com/products-services/simulia/products/cst-studio-suite/>
- [9] F. Schnieder, T. Tischler, and W. Heinrich, “Modeling Dispersion and Radiation Characteristics of Conductor-Backed CPW With Finite Ground Width,” *IEEE Trans. Microwave Theory Tech.*, vol. 51, no. 1, pp. 137–143, Jan. 2003.
- [10] G. N. Phung, F. J. Schmückle, R. Doerner, W. Heinrich, T. Probst, and U. Arz, “Effects Degrading Accuracy of CPW mTRL Calibration at W Band,” in *2018 IEEE/MTT-S International Microwave Symposium - IMS*, 2018, pp. 1296–1299.
- [11] T. K. Johansen, C. Jiang, D. Hadziabdic, and V. Krozer, “EM Simulation Accuracy Enhancement for Broadband Modeling of On-Wafer Passive Components,” in *2007 European Microwave Conference*, 2007, pp. 1245–1248.